

Energy Efficiency of Spread Spectrum Single-Carrier Transmission

Amnart BOONKAJAY[†] Koichi ADACHI^{*} Sumei SUN^{*} and Fumiyuki ADACHI[‡]

^{† ‡} Department of Communications Engineering, Graduate School of Engineering, Tohoku University
6-6-05 Aza-Aoba, Aramaki, Aoba-ku, Sendai, Miyagi, 980-8579 Japan

^{*}Institute for Infocomm Research, A*STAR, 1 Fusionopolis Way, #21-01 Connexis (South Tower), Singapore 138632

E-mail: [†]amnart@mobile.ecei.tohoku.ac.jp ^{*}{kadachi, sunsm}@i2r.a-star.edu.sg [‡]adachi@ecei.tohoku.ac.jp

Abstract Energy efficiency (EE), which is defined as a ratio of spectrum efficiency (SE) to power consumption, is a key performance metric in mobile communication system. The signal waveform has little influence on energy consumption of analog circuit and baseband unit. On the other hand, the energy consumption of power amplifier (PA) highly depends on signal waveform. The power amplifier efficiency (PAE) generally depends on the signal power (equivalently signal amplitude) and decreases as the signal amplitude becomes smaller. If the signal exhibits large peak-to-average power ratio (PAPR), the transmit power needs to be backed off so that the peak signal amplitude is linearly amplified. This results in a poor PAE as the operation point of PA is far below its maximum. The authors previously proposed a single-carrier with frequency domain spread spectrum (SC-FDSS). In this paper, the EE and SE of SC-FDSS are compared to those of SC with conventional time-domain spread spectrum (SC-TDSS). We also observe an optimum spreading factor (SF) for each spreading scheme which gives good SE-EE tradeoff at particular received signal-to-noise power ratio (SNR).

Keyword Spectral efficiency, energy efficiency, power amplifier, single-carrier transmission, spread spectrum

1. Introduction

Broadband wireless channel is characterized as a frequency-selective fading channel, in which inter-symbol interference (ISI) degrades system performance such as bit-error rate (BER) [1]. Although orthogonal frequency division multiplexing (OFDM) eliminates the ISI, its high peak-to-average power ratio (PAPR) property is the main drawback. On the other hand, single-carrier (SC) transmission [2] is more attractive for uplink communication because of its low PAPR. For SC transmission, frequency-domain equalization (FDE) can effectively suppress the adverse impact of ISI [3].

The waveform of SC signal can be manipulated in frequency-domain by inserting discrete Fourier transform (DFT) into conventional OFDM transmitter. The filtering can be done by a one-tap multiplication [4]. The authors have recently proposed a transmission scheme taking advantage of the use of frequency-domain processing called single-carrier with frequency-domain spread spectrum (SC-FDSS) [5].

Unlike the single-carrier time-domain spread spectrum (SC-TDSS) [6], spreading and de-spreading for SC-FDSS are done both in frequency domain by copying and combining frequency components. In [5], SC-FDSS is shown to provide better BER performance than SC-TDSS with the same spreading factor (SF). However, PAPR of SC-FDSS increases as SF increases due to interleaving property of time-domain signal.

Energy efficiency (EE) is recently considered to be a key performance metric in wireless communication system [7]. EE is defined as a ratio of spectrum efficiency (SE) to

power consumption [8]. The power consumption of power amplifier (PA) is considered as a major source [9]. Power consumption of PA normally depends on signal waveform. The signal exhibiting large PAPR leads to poor power amplifier efficiency (PAE) as the operation point of PA is below its maximum. This is because the transmit power requires to be backed off in order to preserve linear amplification.

However, there exists an observation of power consumption and PAE at the low transmit power region. Although low transmit power leads to poor PAE, small amount of amplification power is required. We can also observe from [5] and also in Fig. 1 that there are many points on SC-FDSS waveform which have low transmit power. This implies that lower power consumption of PA in SC-FDSS is possibly achieved at particular target BER even though its PAPR is higher than SC-TDSS.

The above observation motives us to evaluate the SE and EE of SC-FDSS, and then compare them with those of SC-TDSS. An optimum SF for each spreading scheme which gives good SE-EE tradeoff at particular received signal-to-noise power ratio (SNR) is also examined. We expect that better EE is achieved when SC-FDSS is used compared to SC-TDSS with the same SF . Moreover, this indicates that the same performance can be achieved with lower power consumption, implying that SC-FDSS can extend the battery life of mobile terminal (MT), and hence suitable for uplink communication.

The rest of this paper is organized as follows. System models of SC-FDSS and SC-TDSS, including PA, are described in section 2. Section 3 discusses in details of the

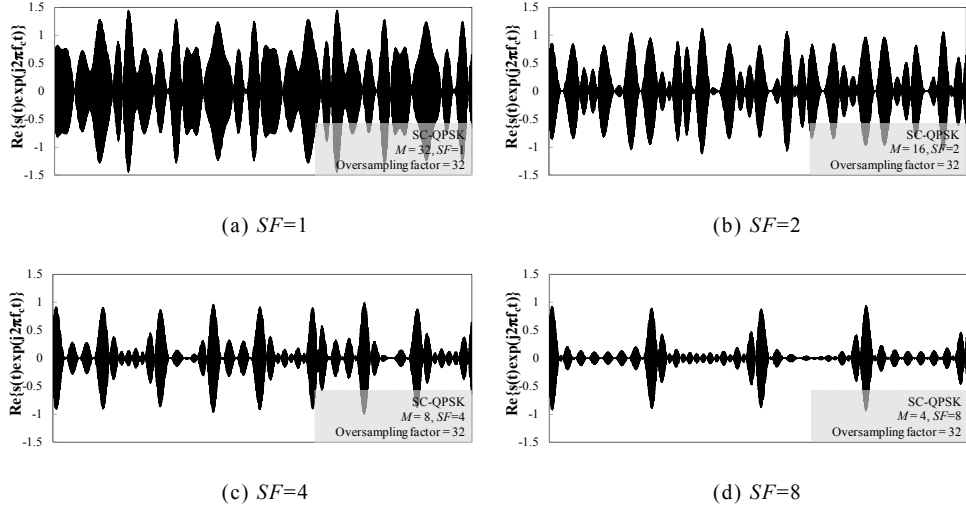


Fig.1 Signal waveforms of SC-FDSS.

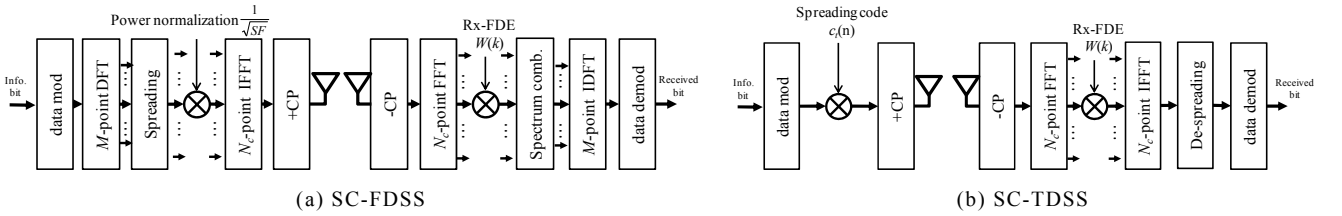


Fig.2 Transmission system models.

definitions of SE and EE. Section 4 shows the performance evaluation, and section 5 concludes the paper.

2. Transmission System Models

Fig. 2 shows the baseband transmission system models of (a) SC-FDSS and (b) SC-TDSS, respectively. We assume single-user transmission of M modulated symbols over available N_c subcarriers, implying that $SF=N_c/M$. N_g -length of cyclic prefix (CP) insertion is also applied.

2.1. SC-FDSS

Let us briefly review the SC-FDSS transmission proposed in [5]. A block of M modulated symbols $\mathbf{d}=[d(0),d(1),\dots,d(M-1)]^T$ is passed through signal processing chain including DFT, frequency-domain spreading, and inverse fast Fourier transform (IFFT). The resultant signal to be transmitted $\mathbf{s}=[s(0),s(1),\dots,s(N_c-1)]^T$ is expressed as

$$\mathbf{s} = \sqrt{\frac{2E_{s,Tx}}{T_s}} \mathbf{F}_{N_c}^H \mathbf{P} \mathbf{F}_M \mathbf{d} = \sqrt{2P_t} \mathbf{F}_{N_c}^H \mathbf{P} \mathbf{F}_M \mathbf{d}. \quad (1)$$

where $E_{s,Tx}$ and T_s represent the transmit symbol energy and symbol duration, respectively. P_t represents the average transmit power. Hermitian transpose of matrix \mathbf{X} is denoted by \mathbf{X}^H and \mathbf{F}_M represents M -point DFT matrix and given by

$$\mathbf{F}_M = \frac{1}{\sqrt{M}} \begin{bmatrix} 1 & 1 & \dots & 1 \\ 1 & e^{-j2\pi(1)(1)/M} & \dots & e^{-j2\pi(1)(M-1)/M} \\ \vdots & \vdots & \ddots & \vdots \\ 1 & e^{-j2\pi(M-1)(1)/M} & \dots & e^{-j2\pi(M-1)(M-1)/M} \end{bmatrix}. \quad (2)$$

The spreading matrix, denoted by \mathbf{P} in (1), is represented by

$$\mathbf{P} = \frac{1}{\sqrt{SF}} \begin{bmatrix} \mathbf{I}_M \\ \mathbf{I}_M \\ \vdots \\ \mathbf{I}_M \end{bmatrix}_{N_c \times M}, \quad (3)$$

where \mathbf{I}_M is an $M \times M$ identity matrix. Before the transmission, the last N_g samples of transmit block are copied as a CP and inserted into the guard interval (GI). The CP-inserted signal block of N_g+N_c samples is transmitted.

After the transmission through wireless channel, the time-domain received signal $\mathbf{r}=[r(0),r(1),\dots,r(N_c-1)]^T$ after CP removal is expressed as

$$\mathbf{r} = \sqrt{2P_r} \mathbf{h} \mathbf{s} + \mathbf{n}, \quad (4)$$

where \mathbf{h} is a circular matrix representing time-domain channel impulse response. The received SNR P_r is determined by

$$P_r = 10^{-\frac{L}{10}} P_t. \quad (5)$$

where L is the pathloss.

After that, \mathbf{r} is transformed into frequency-domain by N_c -point fast Fourier transform (FFT), obtaining the frequency-domain received signal $\mathbf{R} = \mathbf{F}_{N_c} \mathbf{r}$ as

$$\mathbf{R} = \sqrt{2P_r} \mathbf{H}_c \mathbf{P} \mathbf{F}_M \mathbf{d} + \mathbf{N}, \quad (6)$$

where \mathbf{H}_c is a diagonal matrix representing frequency-domain channel response, i.e., $\mathbf{H}_c = \mathbf{F}_{N_c} \mathbf{h} \mathbf{F}_{N_c}^H$.

Joint frequency-domain equalization based on minimum mean-square error criterion (MMSE-FDE) and spectrum combining [10] is employed as frequency-domain de-spreading. Both joint MMSE-FDE and spectrum combining are done by FDE matrix \mathbf{W} with the dimension of $M \times N_c$, which is given as

$$\mathbf{W} = [\mathbf{W}_0 \quad \mathbf{W}_1 \quad \dots \quad \mathbf{W}_{SF-1}], \quad (7)$$

where \mathbf{W}_n is an $M \times M$ diagonal matrix expressed by

$$\mathbf{W}_n = \text{diag} \left[W \left(\frac{(nSF)M}{SF} \right), W \left(\frac{(nSF)M}{SF} + 1 \right), \dots, W \left(\frac{((n+1)SF)M}{SF} + 1 \right) \right]. \quad (8)$$

Here, $W(k)$ is represented by

$$W(k) = \frac{1}{\sqrt{SF}} H_c^*(k) \frac{1}{\frac{1}{SF} \sum_{g=0}^{SF-1} |H_c(k \bmod M + gM)|^2 + \left(\frac{E_{s,Rx}}{N_0} \right)^{-1}}, \quad (9)$$

where $H_c(k)$ is the elements in \mathbf{H}_c with respect to each frequency index. $E_{s,Rx}$ represents the received symbol energy. The frequency-domain received signal after equalization and spectrum combining $\hat{\mathbf{D}} = \mathbf{W} \mathbf{R}$ is finally transformed back into time-domain by M -point inverse DFT (IDFT). Therefore, the time-domain received signal after de-spreading $\hat{\mathbf{d}} = [\hat{d}(0), \hat{d}(1), \dots, \hat{d}(M-1)]^T$ is given by

$$\hat{\mathbf{d}} = \mathbf{F}_M^H \hat{\mathbf{D}} = \mathbf{F}_M^H \mathbf{W} \mathbf{R}. \quad (10)$$

2.2. SC-TDSS

In this paper, SC-TDSS proposed in [6] is considered as a benchmark. The time-domain signal to be transmitted before adding guard interval $\mathbf{s} = [s(0), s(1), \dots, s(N_c-1)]^T$ is given by

$$s(n) = \sqrt{\frac{2E_{c,Tx}}{T_s}} d \left(\left\lfloor \frac{n}{SF} \right\rfloor \right) c_i(n \bmod SF), \quad (11)$$

where $E_{c,Tx}$ represents transmit chip energy as $E_{c,Tx} = E_{s,Tx} / SF$. $c_i(n)$ represents spreading code generated from 4095-bit long pseudo-noise (PN) sequence. After CP insertion, transmission, and CP removal at the receiver, the time-domain received signal $\mathbf{r} = \sqrt{2P_r} \mathbf{h} \mathbf{s} + \mathbf{n}$ is transformed to frequency domain, obtaining

$$\mathbf{R} = \sqrt{2P_r} \mathbf{H}_c \mathbf{S} + \mathbf{N}. \quad (12)$$

Here, $\mathbf{S} = \mathbf{F}_{N_c} \mathbf{s}$ is frequency-domain transmitted signal.

MMSE-FDE weight matrix $\mathbf{W} = \text{diag}[W(0), \dots, W(N_c-1)]$ is applied to the frequency-domain received signal \mathbf{R} . The FDE weight $W(k)$ is given by

$$W(k) = \frac{H_c^*(k)}{|H_c(k)|^2 + (E_{c,Rx} / N_0)^{-1}}. \quad (13)$$

After applying the FDE, the signal is transformed back into time-domain as $\tilde{\mathbf{d}} = \mathbf{F}_{N_c}^H \mathbf{W} \mathbf{R}$. The time-domain signal before demodulation $\hat{\mathbf{d}} = [\hat{d}(0), \hat{d}(1), \dots, \hat{d}(M-1)]^T$ is obtained by time-domain de-spreading, which is

$$\hat{d}(n) = \frac{1}{SF} \sum_{t=nSF}^{(n+1)SF-1} \tilde{d}(t) c_i^*(t). \quad (14)$$

2.3. Power Amplifier Model

Since this paper is focusing on uplink communication. Class-B power amplifier, which is suitable for MT, is considered with particular amplifying gain g . The PAE is defined as the ratio of the output power to the total required power. The PAE formula is calculated as [11]

$$\eta = \frac{P_{out}}{P_{DC}} = \frac{\pi}{4} \sqrt{\frac{P_{out}}{P_{out}^{\max}}}, \quad (15)$$

where P_{out} and P_{out}^{\max} represent output power and maximum output power, respectively. From (15), instantaneous power consumption of the PA, P_{DC} , is expressed by

$$P_{PA} = \frac{4}{\pi} \sqrt{P_{out}^{\max} P_{out}}. \quad (16)$$

It is observed from (15) that the highest PAE is reached when the operating point is at the maximum output power. However, the PA has to be backed off by at least the amount of PAPR for preserving linear amplification. Thus, the instantaneous power consumption of PA at time instance n can be rewritten as [11]

$$P_{PA} = \frac{4}{\pi} \sqrt{\xi \cdot P_{out}^{\max} \bar{P}_{out}} \frac{|s(n)|}{\max\{|s(n)|\}}, n = 0, 1, \dots, VN_c - 1 \quad (17)$$

Here, V represents an oversampling factor and ξ is the PAPR value. \bar{P}_{out} is average transmit power. It can be noted from (16) that the power consumption of class-B PA depends on the envelope of transmit signal.

3. SE and EE

The SE is normally defined in bps/Hz, i.e., the amount of information bits that are reliably received per unit frequency. The SE (bps/Hz) is computed as [12]

$$SE = N_{\text{mod}} (1 - \text{PER}) \left(\frac{1}{SF} \right) \left(\frac{1}{1 + N_g / N_c} \right), \quad (18)$$

where N_{mod} is modulation level, and PER is packet-error rate.

The EE is defined as the ratio of the total throughput divided by the total required power. Thus, EE in bits per joule (b/J) is expressed by

$$EE = \frac{W \times SE}{P_c}, \quad (19)$$

where W is the total transmission bandwidth, and P_c represents total power consumption. The total power consumption P_c is decomposed into [13]

$$P_c = P_{PA} + 2P_{\text{mix}} + 2P_{FS} + 2P_{LNA} + P_{\text{filter}} + P_{BA} + P_{ADC} + P_{DAC}, \quad (20)$$

where P_{PA} is power consumption of PA given in (17). P_{mix} , P_{FS} , P_{LNA} , P_{filter} , P_{BA} , P_{ADC} , and P_{DAC} are power consumption of mixer, frequency synthesizer, low-noise amplifier (LNA), analog filters, baseband amplifier, analog-to-digital converter (ADC), and digital-to-analog converter (DAC), respectively. Except for P_{PA} , the power consumption of each component is independent of signal waveform, and hence, they can be simply considered as constant power.

Table 1 Simulation parameters.

| Transmitter | Data modulation | QPSK |
|-----------------|----------------------|--|
| | FFT/IFFT block size | $N_c = 256$ |
| | Cyclic prefix length | $N_g = 32$ |
| | Spreading factor | $SF=1\sim 16$ |
| Power amplifier | Amplifier type | Class-B |
| | Maximum output power | $P_{\text{out}}^{\text{max}} = 13$ dBm |
| Channel | Fading | Frequency-selective block Rayleigh |
| | Power delay profile | 16-path uniform power delay profile |
| | AWGN power density | $N_0 = -174$ dBm/Hz |
| | Distance | $R = 500$ m |
| Total bandwidth | 2.5 MHz | |
| Receiver | Channel estimation | Ideal |

Table 2 RF power consumption for each component.

| | |
|---------------------|---------|
| P_{mix} | 21 mW |
| P_{FS} | 67.5 mW |
| P_{LNA} | 20 mW |
| P_{filter} | 5 mW |
| P_{BA} | 5 mW |
| P_{ADC} | 7.8 mW |
| P_{DAC} | 27.4 mW |

4. Performance Evaluation

Numerical and simulation parameters are summarized in Table 1. We assume quadrature phase shift keying (QPSK) block transmission with the number of subcarriers $N_c=256$. Performance of those transmission schemes, i.e. SC-FDSS and SC-TDSS, is evaluated in terms of SE, power consumption, and EE. Performance evaluation of EE is done at target average received SNR is 10 dB. Here, the average received SNR is defined regarding to the noise power spectrum density defined in Table 1. For example,

in case of the received SNR=10 dB, the average received signal power is 10 times of $N_0 \times W$. We assume the pathloss L (in dB) according to macro-cell model at the operating frequency of 2 GHz which is given as [14]

$$L = 128.1 + 37.6 \log_{10}(R), \quad (21)$$

where R is communication distance (in kilometer).

4.1. SE Performance

The SE (bps/Hz) of SC-FDSS and SC-TDSS in various SF is shown in Fig. 3. The performances at average received SNR of 10 dB and 15 dB are considered.

Fig. 3 shows that SC-FDSS and SC-TDSS provide almost the same SE at high- power region (SNR=15dB) as they reach the maximum throughput. The SE of SC-FDSS is higher than that of SC-TDSS for given SF due to the improvement of BER.

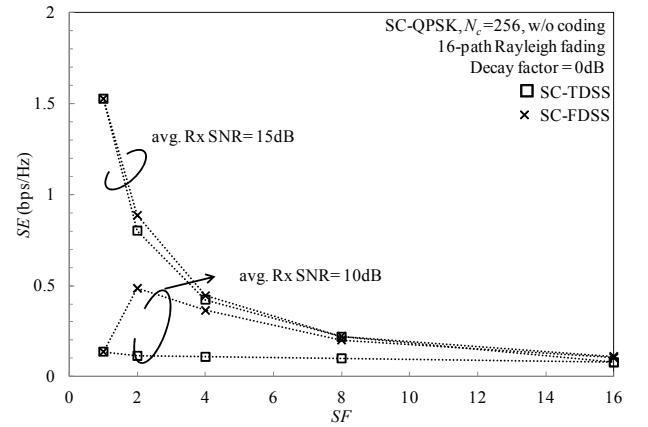


Fig.3 SE performance of SC-FDSS and SC-TDSS

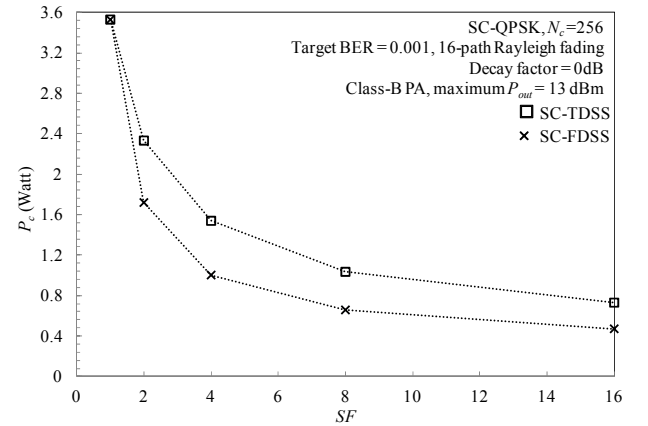


Fig.4 Power consumption at the target received SNR is 10 dB.

4.2. Power Consumption of PA

The power consumption of PA, which is defined as the average of the instantaneous power consumption calculated in (20), is shown in Fig. 4. The target average received SNR is set to 10 dB. From the figure, SC-FDSS requires less power consumption compared to SC-TDSS for every SF . This is because there are many points on

SC-FDSS waveform which have low transmit power especially when SF increases, and hence leads to lower power consumption compared to SC-TDSS.

4.3. EE Performance

The EE performances of SC-FDSS and SC-TDSS with the average received SNR of 10 dB are plotted as a function of SF in Fig. 5. It is observed that SC-FDSS gives better EE compared to SC-TDSS irrespective of SF . We can also observe that the EE increases as SF increases for SC-TDSS, where the EE decreases when $SF > 4$ for SC-FDSS. This phenomenon can be explained as follows. The signal waveform of SC-FDSS becomes more comb-like shape as SF increases. This implies that the more time instances the power consumption of PA becomes less. However, it is also observed from Fig. 3 that the SE decreases because it reaches the maximum throughput when $SF > 4$, leading to the decrease of EE even though the power consumption decreases.

In addition, SE-EE tradeoff is evaluated as shown in Fig. 6. It can be observed the EE improves as SF increases until $SF=4$ for SC-FDSS, and then turns to decrease from $SF=8$ due to the decrease of EE. Regarding to this, it can be concluded that the optimal SF which gives the best EE for SC-FDSS is 4.

5. Conclusion

In this paper, we evaluated the performance of two spread spectrum techniques, i.e. SC-FDSS and SC-TDSS, in terms of spectrum efficiency (SE), power consumption, and energy efficiency (EE). The power consumption of PA is also included. The simulation results confirmed that SC-FDSS gives better SE when comparing with SC-TDSS at the same SF when the average received SNR is low. It is also confirmed that SC-FDSS provides better EE for a given SE when SF is no larger than 16.

References

- [1] A. Goldsmith, *Wireless Communications*, Cambridge University Press, 2005.
- [2] H. G. Myung, J. Lim, and D. J. Goodman, "Single Carrier FDMA for Uplink Wireless Transmission", *IEEE Veh. Mag.*, vol.1, pp.30-38, Sept. 2006.
- [3] D. Falconer, S. Ariyavisitakul, A. Benyamin-Seeyar, and B. Eidson, "Frequency Domain Equalization for Single-Carrier Broadband Wireless Systems," *IEEE Commun. Mag.*, vol.40, no.4, pp. 58-66, April 2002.
- [4] K. Takeda and F. Adachi, "Joint Iterative Transmit/Receive FDE&FDIC for Single-Carrier Block Transmissions," *IEICE Trans. Commun.*, vol. E94-B, no. 5, pp. 1396-1404, May 2011.
- [5] A. Boonkajay, T. Obara, T. Yamamoto, and F. Adachi, "Generalized Frequency-Domain Filtered Single-Carrier Transmission", *IEICE Technical Report*, RCS2012-320, pp.219-224, March 2013.
- [6] K. Takeda and F. Adachi, "Performance Evaluation of Multi-Rate DS-SS-CDMA Using Frequency-Domain Equalization in a Frequency-Selective Fading Channel," *IEICE Trans. Commun.*, vol.E88-B, no.3, March 2005.
- [7] J. Joung, C. K. Ho, and S. Sun, "Spectral Efficiency and Energy Efficiency of OFDM Systems: Impact of Power Amplifiers and Countermeasures," to be published in *IEEE J. Sel. Areas. Commun.*, 2013.
- [8] C. Isheden and G. P. Fettweis, "Energy-Efficient Multi-Carrier Link Adaptation with Sum Rate-Dependent Circuit Power," in *Proc. IEEE Global Commun. Conf. (Globecom)*, Dec. 2010.
- [9] H. Bogucka and A. Conti, "Degree of Freedom for Energy Savings in Practical Adaptive Wireless Systems," *IEEE Commun Mag.*, vol.49, pp.38-45, Jun. 2011.
- [10] T. Obara, K. Takeda, and F. Adachi, "Joint Frequency-Domain Equalization and Spectrum Combining for the Reception of SC Signals in the Presence of Timing Offset," in *Proc. IEEE Veh. Technol. Conf. (VTC) 2010-Spring*, May 2010.
- [11] M. Talonen and S. Lindfors, "Power Consumption Model for Linear RF Power Amplifiers with Rectangular M-QAM Modulation," in *Proc. IEEE Int. Symp. on Wireless Commun. Syst. (ISWCS)*, Oct. 2007.
- [12] K. Fukuda, A. Nakajima, and F. Adachi, "LDPC-coded HARQ Throughput Performance of MC-CDMA using ICI Cancellation," in *Proc. IEEE Veh. Technol. Conf. (VTC) 2007-Fall*, Sept. 2007.
- [13] Y. Li, B. Bakaloglu, and C. Chakrabarti, "A System Level Energy Model and Energy-Quality Evaluation for Integrated Transceiver Front-Ends," *IEEE Trans. VLSI Syst.*, vol.15, no.1, pp.90-103, Jan 2007.
- [14] "LTE; E-UTRA; RF requirements for LTE Pico node B," ETSI, Tech. Rep. 136 931 V9.0.0, 2011.

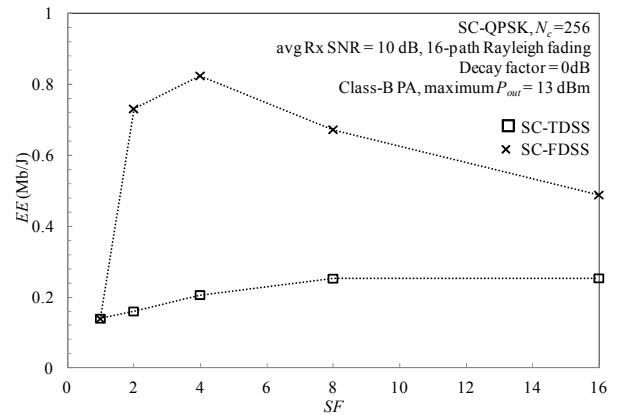


Fig.5 EE performance as a function of SF.

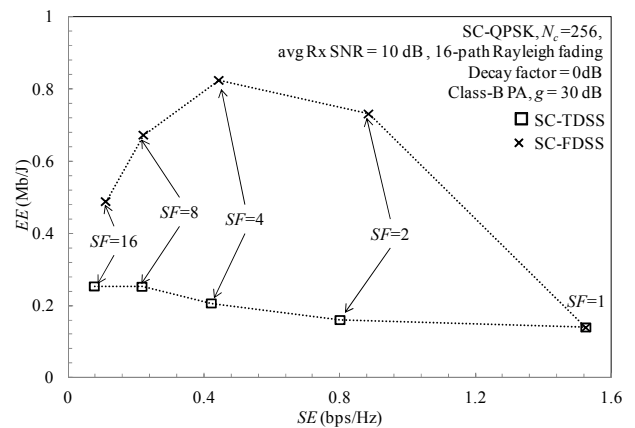


Fig.6 SE-EE tradeoff.